International journal of spray and combustion dynamics

Original Research Article

International Journal of Spray and Combustion Dynamics
2017, Vol. 9(4) 367–379

DOI: 10.1177/1756827716687583
journals.sagepub.com/home/scd
SAGE

Uncertainty encountered when modelling self-excited thermoacoustic oscillations with artificial neural networks

Stefan Jaensch and Wolfgang Polifke

Abstract

Artificial neural networks are a popular nonlinear model structure and are known to be able to describe complex nonlinear phenomena. This article investigates the capability of artificial neural networks to serve as a basis for deducing nonlinear low-order models of the dynamics of a laminar flame from a Computational Fluid Dynamics (CFD) simulation. The methodology can be interpreted as an extension of the CFD/system identification approach: a CFD simulation of the flame is perturbed with a broadband, high-amplitude signal and the resulting fluctuations of the global heat release rate and of the reference velocity are recorded. Thereafter, an artificial neural network is identified based on the time series collected. Five data sets that differ in amplitude distribution and length were generated for the present study. Based on each of these data sets, a parameter study was conducted by varying the structure of the artificial neural network. A general fit-value criterion is applied and the 10 artificial neural networks with the highest fit values are selected. Comparing of these 10 artificial neural networks allows to obtain information on the uncertainty encountered. It is found that the methodology allows to capture the forced response of the flame reasonably well. The validation against the forced response, however, depends strongly on the forcing signal used. Therefore, an additional validation criterion is investigated. The artificial neural networks are coupled with a thermoacoustic network model. This allows to model self-excited thermoacoustic oscillations. If the training time series are sufficiently long, this coupled model allows to predict the trend of the root mean square values of fluctuations of the global heat release rate. However, the prediction of the maximal value of the fluctuation amplitude is poor. Another drawback found is that even if very long-time series are available, the behaviour of artificial neural networks cannot be guaranteed. It is concluded that more sophisticated nonlinear low-order models are necessary.

Keywords

System identification, nonlinear flame dynamics, laminar premixed flames, self-excited thermoacoustic oscillations, artificial neural networks

Date received: 25 April 2016; accepted: 12 December 2017

1. Introduction

Thermoacoustic oscillations limit the development of gas turbines and rocket engines. These oscillations are nonlinear. Hence, in order to decide whether or not a thermoacoustic oscillation reaches critical amplitude levels, nonlinear low-order models are necessary.

Several models have been developed to predict these amplitude levels. The flame describing function (FDF) combined with a one-dimensional model for the acoustics has been proven to give useful estimates of the oscillation amplitudes in many cases.[1–3] It is also possible to deduce an FDF from a CFD simulation.[4–6] The FDF is limited to harmonic oscillations, where higher harmonics in the flame response are unimportant. As shown by Moeck and Paschereit[7] and Orchini et al.,[8] the FDF can be extended to the so-called flame double input describing function (FDIDF). This increases the accuracy of the prediction significantly. However, determining a FDIDF is

Technische Universität München, Fakultät für Maschinenwesen, Garching, Germany

Corresponding author:
Stefan Jaensch, Technische Universität München, Fakultät für Maschinenwesen, D-85747 Garching, Germany.
Email: Jaensch@tfd.mw.tum.de

prohibitively expensive for practically relevant applications.[8] Another model that has drawn recent interest is the G-equation.[2,8–11] The drawback of G-equation-based models is that the results depend strongly on the velocity model used. Consequently, no quantitative agreement with experiment is obtained. A promising technique is hybrid CFD/low-order models.[12–16] These models have the advantage that they can account for the complex interaction between heat source, flow and acoustics. Additionally, compared to a fully compressible simulation of the whole thermoacoustic configuration, the computational effort can be significantly reduced. However, the computational effort is still high and more efficient non-linear low-order models are needed. A general methodology for deriving low-order models from a CFD simulation is the CFD/system identification (SI) approach.[17] The general idea of the CFD/SI approach is to force a CFD simulation with broadband excitation signal. If the flame dynamics of a premixed flame is to be determined, the resulting fluctuation of the reference velocity and of the global heat release rate is recorded. From these time series low-order models can be deduced by system identification.[18,19] In the linear regime, the CFD/SI approach is known to yield accurate estimates of the flame transfer function (FTF).[17] The CFD/SI approach can be extended to the nonlinear regime.[18,20] Selimefendigil et al.[21–23] used the method to identify nonlinear low-order models for a cylinder in pulsating crossflow. Zhang et al.[24] used Hammerstein–Wiener models to deduce nonlinear low-order models from a G-equation solver.

In the present study, the CFD/SI approach is used to obtain nonlinear low-order models of a laminar flame. The capability of artificial neural networks (ANNs) to serve as the nonlinear model structure is investigated. ANNs have become a very popular black-box model in the last decades. They have been used to predict stock prices to forecast the weather and to model aircrafts. The ANN framework provides a model structure, which can easily be extended in such a way that very complex nonlinearities can be described. Consequently, it is expected that there exists an ANN that describes the nonlinear flame dynamic accurately. Indeed, Blonbou et al.[25,26] and Vaudrey and Saunders[27] showed that ANNs can be used to control combustion instabilities. However, the model structure of an ANN has a large number of parameters and consequently, ANNs are prone to over-fitting. This phenomenon occurs in particular if only short time series are available. In contrast to experimental test rigs, as investigated by Blonbou et al.[25,26] and Vaudrey and Saunders,[27] the time series used for the CFD/SI approach should be as short as possible. Otherwise, no advantage in computational time can be achieved. Therefore, the key question addressed in the present study is whether or not an appropriate ANN can be determined based on the limited information available, i.e. the broadband time series. An ANN is considered to be appropriate if on the one hand it can capture the forced response of the flame. This criterion allows to validate the predicted fluctuation of the global heat release rate in both the time and the frequency domain in a straightforward manner. A drawback of this comparison is that it depends strongly on the forcing signal used. Therefore, on the other hand, an additional validation criterion is investigated. The ANNs identified are combined with a thermoacoustic network model in order to model self-excited thermoacoustic oscillations. The predicted oscillations are compared against the results obtained with the hybrid CFD/low-order models discussed in Jaensch et al.[16] This validation analyses if small errors made by the ANN accumulate and is very close to the application considered. A difficulty of this validation is that thermoacoustic oscillations can be very complex, which makes a direct comparison in the time or frequency domain difficult. In the present study, we compare the oscillations predicted in terms of root mean square (RMS)-values and the maximal fluctuation of the global heat release rate.

In the next section, the CFD setup is introduced, which forms the basis of the present study. Thereafter, we discuss how ANNs can be used for the CFD/SI approach. Then, the methodology is validated in terms of forced response and self-excited oscillations.

2. Numerical setup

The CFD setup is shown in Figure 1 and corresponds to the multi-slit burner investigated by Kornilov et al.[28]

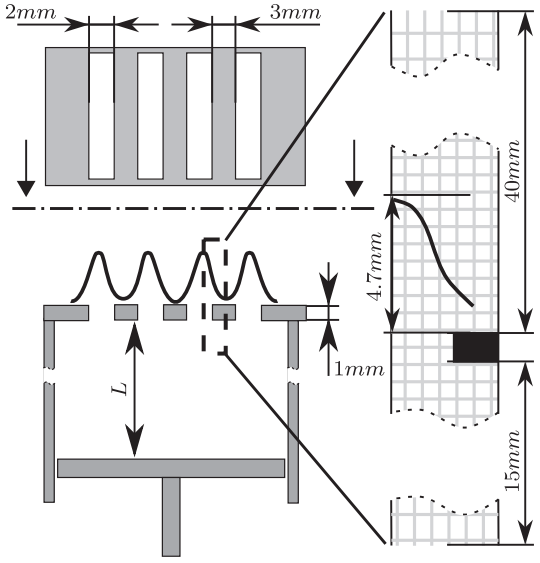

Figure 1. Multi-slit burner and the corresponding CFD domain investigated.[16]

and Duchaine et al.[29] The numerical settings were chosen as in Duchaine et al.,[29] i.e. equivalence ratio 0.8, inlet velocity 0.4 m/s, inlet temperature, 293 K and wall temperature 373 K. In contrast to Duchaine et al.,[29] a low Mach formulation of the Navier–Stokes equations was solved. This implies that the density depends on the temperature only, but not on the pressure. Consequently, the acoustics inside the computational domain is suppressed. In particular, this modification also suppresses the intrinsic thermoacoustic feedback.[30] It is expected that this simplifies the identification significantly, it allows us to investigate an open-loop problem. OpenFOAM (http://www.openfoam.org/) was used as CFD solver. The CFD setup used in the present study is identical to the low-Mach simulation described in Jaensch et al.[16]

3 ANNs

In the present section, first the structure of ANNs is introduced. Afterward, it is discussed how ANNs can be used as a nonlinear model structure for the CFD/SI approach.

3.1. Structure of ANNs

An ANN consists of interconnected *neurons*. A single neuron is a function $y = \sigma(\mathbf{u}, \boldsymbol{\Theta})$ with input vector $\mathbf{u}$ and a scalar output y. $\boldsymbol{\Theta}$ is the parameter vector. The function $\sigma(\cdot)$ is called the activation function. In principle, any function can be used. For practical applications, sigmoid functions and radial basis functions (RBF) have been proven to be useful choices.[20;18] Examples of both functions plotted in Figure 2. A sigmoid function is given as

$$\sigma_{\mathrm{Sig}}(\mathbf{u}, \boldsymbol{\Theta}) = \frac{2}{1 + \exp\left(-2\boldsymbol{\Theta}^T \mathrm{u}\right)} - 1 \tag{1}$$

Here, the parameter vector $\boldsymbol{\Theta}$ weights the inputs. Consequently, the elements Θ_k of $\boldsymbol{\Theta}$ are called *weights*. A radial basis function is defined as

$$\sigma_{\mathrm{RBF}}(\mathbf{u},\ \mathrm{c},\ \Sigma) = \exp\left(-\frac{1}{2}\|\mathbf{u} - \mathrm{c}\|_{\Sigma}^2\right) \tag{2}$$

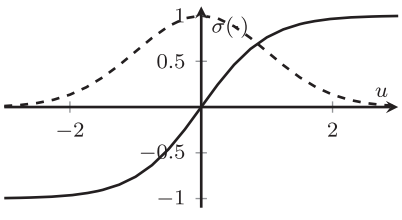

Figure 2. Full line: sigmoid function with $\Theta = 1$, dashed line: radial basis function (RBF) with $\sum = 1$ and $c = 0$.

with the generalized norm

$$\|\mathbf{u} - \mathrm{c}\|_{\Sigma} = \sqrt{(\mathbf{u} - \mathrm{c})^T\ \Sigma(\mathbf{u} - \mathrm{c})} \tag{3}$$

Here, the parameter vector $\boldsymbol{\Theta}$ is represented by the centre vector c and the norm matrix . These quantities correspond to the mean vector and the covariance matrix of a multivariate normal distribution. In order to reduce the number of parameters, Σ is assumed to be a diagonal matrix.

Several interconnected neurons build an ANN. As depicted in Figure 3, ANNs are structured in several layers. The inputs of the ANN are time-lagged velocity signals $u'(t - i\Delta t)$. Here, i is the time increment and Δt is the time step. The inputs of the ANN are also the inputs of the neurons positioned in the first layer. The inputs of the neurons in the second layer are the outputs of the neurons in the first layer and so on. The last layer consists of a single neuron with a linear activation function. Note that all neurons positioned in the same layer have the same inputs. As only time-lagged input signals and no time-lagged output signals are the inputs of the ANN the impulse response of the ANNs considered is finite and has the length $n\Delta t$. An infinite impulse response would require us to pass the output of the ANN as feedback to its inputs. This is analogue to a finite impulse response (FIR) model used for linear system identification. The finiteness of the impulse response reflects the convective nature of the flame dynamics: an impulse velocity perturbation impinging on the flame causes a perturbation of the flame front and consequently a fluctuation of the global heat release rate. Blumenthal et al.[31] showed for a G-equation flame model that the perturbation of the flame front is convected through the flame and that the original flame front is restored via a convective

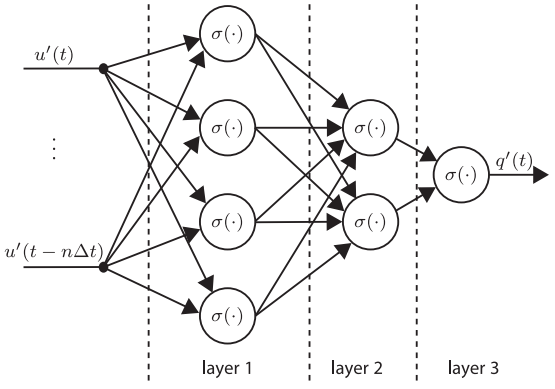

Figure 3. Generic example of a structure of an artificial neural network with four neurons in the first layer, two neurons in the second layer and a single neuron in the third layer.

restoration mechanism. Once the perturbation and the restoration are convected through the flame, the fluctuation of the global heat release vanishes instantaneously. Thus the impulse response of the flame is finite. Therefore, the FIR model should be considered as a grey-box model of the flame.[32] It is expected that these considerations hold for the nonlinear flame dynamics. In general, the ANN framework allows to additionally consider time-lagged values of the output signal, i.e. the fluctuation of the global heat release rate, as inputs of to the neural network. However, this yields an oscillatory impulse response, which does not correspond to the convective nature of the flame response. Silva et al.[33] show that these so-called *auto-regressive* models are useful for modeling the scattering matrix of a flame, but not for the FTF.

Typically, all activation functions of neurons positioned in the same layer are identical. If RBFs are used, it is advantageous to normalize the output of the k-th neuron in a layer by the output of all neurons in the same layer

$$\sigma_{\mathrm{NRBF},k}(\mathbf{u}, \mathrm{c}, \Sigma) = \frac{\sigma_{\mathrm{RBF}}(\mathbf{u}, \mathrm{c}_k, \Sigma_k)}{\sum_{i=0}^{M} \sigma_{\mathrm{RBF}}(\mathbf{u}, \mathrm{c}_i, \Sigma_i)} \tag{4}$$

with M being the number of neurons in the layer. The function $_{\mathrm{NRBF;k}}(\mathrm{u}, \mathrm{c}, \Sigma)$ is called *normalized radial basis function* (NRBF).

3.2. Identification of ANNs

The identification procedure used to determine the unknown parameter vector $\boldsymbol{\Theta}$ of an ANN is similar to the procedure used for linear identification[17,18]:

1. First, a broad band time series is created.
2. The model structure has to be chosen.
3. The unknown parameters are determined by solving an optimization problem.
4. The model identified must be validated.

In order to generate broad band time series, the CFD simulation introduced above was forced with different broadband excitation signals. The signals were generated with the method discussed in Föller and Polifke.[34] As for the linear CFD/SI approach, the frequency content of the signal should be chosen such that all frequencies of interests are excited. For the nonlinear identification, also the amplitude of the signal is important. Therefore, signals with different amplitudes are investigated in the present study. The particular signals used are discussed in detail in the next section.

The second step of the identification procedure is to fix the structure of the ANN. This means choosing the activation function, the number of layers and the number of neurons per layer. Additionally, the maximum delay n has to be fixed. Unfortunately, there exist no general design rules for choosing the structure of an ANN. Typically, one identifies several ANNs with different structures and selects the ANN with the best performance. In the present study, this is done in terms of a large parameter study, which is discussed in the next section.

The third step of the identification procedure is to determine the vector of unknown parameters $\boldsymbol{\Theta}$ of the neural networks. This is done by solving the optimization problem

$$\min_{\boldsymbol{\Theta}} \frac{1}{N} \sum_{i=0}^{N-1} \left(q'_{\mathrm{ANN}}(i\Delta t,\ \boldsymbol{\Theta}) - q'_{\mathrm{CFD}}(i\Delta t) \right)^2 \tag{5}$$

This optimization problem is nonlinear and consequently, nonlinear optimization algorithms are necessary. These algorithms are based on error backpropagation, which allows to calculate the gradient of the cost function analytically. In comparison to the Wiener–Hopf inversion, the computational effort required is significantly larger. However, compared to the computational costs of the CFD simulation, the computational effort is still negligible. A particularity of ANNs is that the optimization is non-deterministic. Recall from the discussion of the structure of ANNs that the inputs and outputs of all neurons positioned in the same layer are equal (see also Figure 3). Hence, neurons positioned in the same layer differ only with respect to their parameter vector. Consequently, if in order to solve the optimization problem all parameters are initialized to zero, after the optimization the parameters of all neurons positioned in the same layer will be equal. The performance of such an ANN would be poor. In order to avoid this behaviour, the parameter vector is initialized to small, random values. Consequently, re-identifying an ANN with the same structure several times can yield ANNs, showing a significantly different performance. Note that only the optimization algorithm is non-deterministic. ANNs are a deterministic model once all parameters have been determined. The number of unknown parameters of an ANN grows rapidly with the number of neurons and layers. This enables ANNs to model complex nonlinearities, however, it creates the risk of over-fitting. If the optimization problem (5) is solved untill convergence, the quality of the ANN obtained would be poor. In order to avoid over-fitting, the data used to identify the parameters of the ANNs is divided into three different data sets: training data, validation data and test data. The optimization algorithm calculates the gradient of the cost function using only the training data set. The optimization stops when the

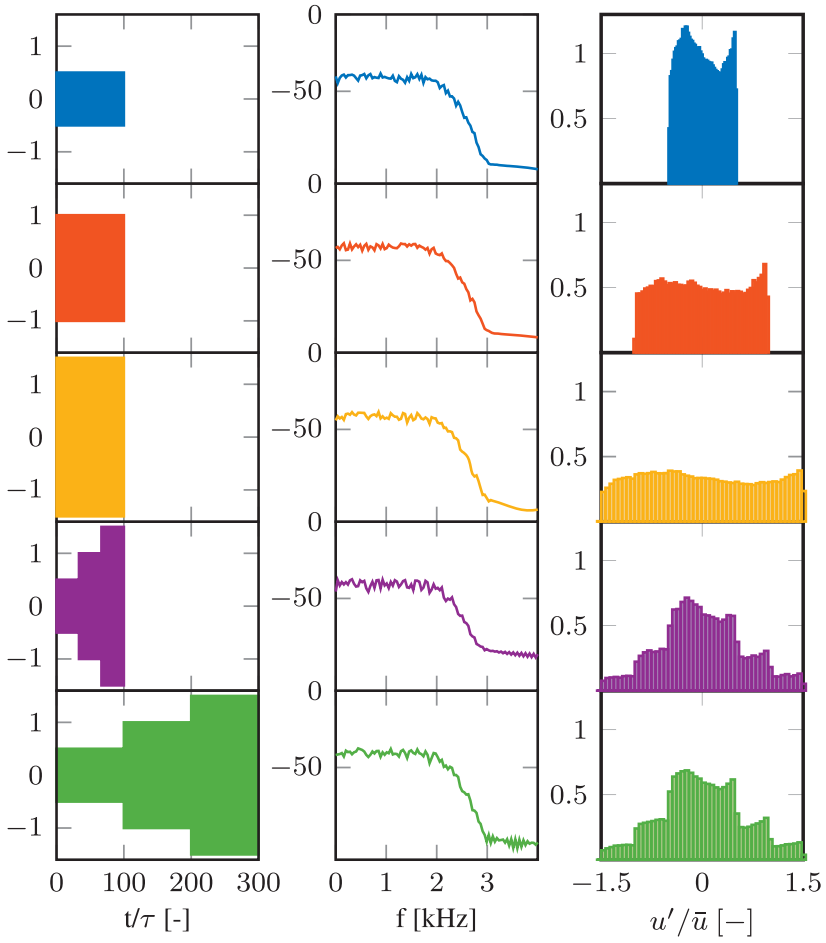

Figure 4. Five different data sets used to generate the ANNs. Left: envelope of the time series $u'/\bar{u}[-]$, middle: power spectral density PSD (dB/Hz), right: empirical probability density function.

error made on the validation data set increases. The test data set is not used during the optimization. In the present work, 70% of the data are used as training data, 15% as validation data and 15% as test data. The data were divided randomly using a fixed seed.

For the present study, the default implementation of ANNs in Matlab (www.mathworks.com, version: R2015b) is used.

4. Numerical results

Unfortunately, there are no general design rules for the structure of neural networks. Indeed, as the training of neural networks is non-deterministic, two ANNs with the same structure can show totally different behaviour. This holds even if the same data set was used to train both networks. In order to use ANNs to model self-excited thermoacoustic oscillations a criterion is necessary, which allows to decide whether or not an ANN identified is a good low-order model of the nonlinear flame dynamics. This criterion should be based on the broadband time series used to identify the network. Otherwise, the computational effort required to find a suitable ANN can make the methodology prohibitively expensive. The criterion investigated in the present work is the fit value defined as

$$\text{fit} = 100\left(1 - \frac{\|q'_{\text{CFD}} - q'_{\text{ANN}}\|}{\|q'_{\text{CFD}} - q'_{\text{CFD}}\|}\right) \tag{6}$$

with the temporal average q'_{CFD} of the fluctuations of the global heat release rate measured in the CFD simulation. This criterion is also known as normalized root mean square error (NRMSE). The criterion is evaluated using the full broadband time series including training data, validation data and test data. Recall that the weights of the ANN are determined via the optimization procedure discussed in the previous section using the validation and the training data. The test data are not used. Considering this data to select the optimal ANNs is an additional method to prevent over-fitting.

In order to increase the generalizability of the results of the present study, a large number of ANNs with different structures were identified using the five data

sets shown in Figure 4. The 10 ANNs with the greatest fit values on each data set were selected. The underlying parameter study is explained in detail in the next subsection. Thereafter, the ANNs selected are validated against the forced response and against self-excited thermoacoustic oscillations.

4.1. Setup of the parameter study

As shown in Figure 4, five different broadband time series are investigated. These data sets were generated by forcing the inflow velocity u' of the CFD simulation with three different broadband excitation signals. The length of the time series obtained is $100\,\tau$. Here, τ is the length of the impulse response of the flame and is equal to 10 ms. All signals are statistically independent from each other and were generated with the non-Gaussian simulation method described in Föller and Polifke.[34] A small part of the signal is shown in Figure 7. The signals were scaled such that the amplitude $u'/\bar{u}$ of the first signal is 50%, the one of the second signal is 100% and the one of the third signal is 150%. From the three time series obtained, five different data sets were generated. These data sets are shown in Figure 4. The data sets 1, 2 and 3 are the time series directly generated by the CFD simulation. Data set 4 is concatenated and consists of the first third of the data sets 1 to 3, respectively. Data set 5 is concatenated and consists of the full data sets 1 to 3. Data set 4 and 5 are investigated in to analyse whether signals containing several excitation amplitude levels can improve the results. In the linear regime, the length of the time series and its power spectral density are sufficient to characterize the excitation signal used for identification. This is because linearity implies that the response is independent from the excitation amplitude. In the nonlinear regime, however, also the distribution of the amplitudes is important. In Figure 4, this is shown by the empirical probability density function.

In addition to the time series, also the structure of the ANN is varied. The parameters changed are listed in Table 1. All 3780 combinations of these parameters

Table 1. Parameters varied for the parameter study.

$\Delta t/\tau$	0.015, 0.03, 0.06
$n\Delta t/\tau$	1.5, 2, 2.5
# neurons	2 to 20 (step size of 2)
# layers	2, 3
σ (–)	Sigmoid, NRBF

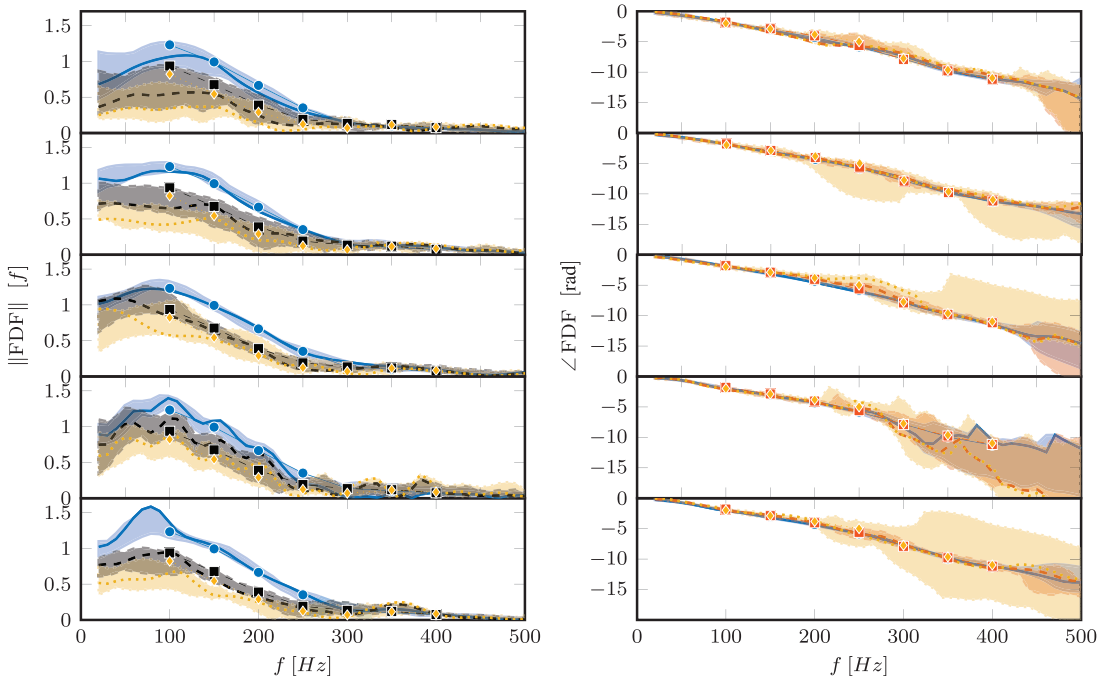

Figure 5. Comparison of the FDF deduced from the optimal ANNs and from the CFD simulation. Left: gain; right: phase; lines: estimate by the ANN with the highest fit value. Shaded area: bounds of the prediction made by the 10 optimal ANNs selected. Markers: reference generated by forcing the CFD with harmonic signals. Excitation amplitudes: A = 50% (full blue line, blue dots), A = 100% (dashed black line, black squares), A = 150% (dotted yellow line, yellow diamonds), training data sets ordered top to bottom as in Figure 4.

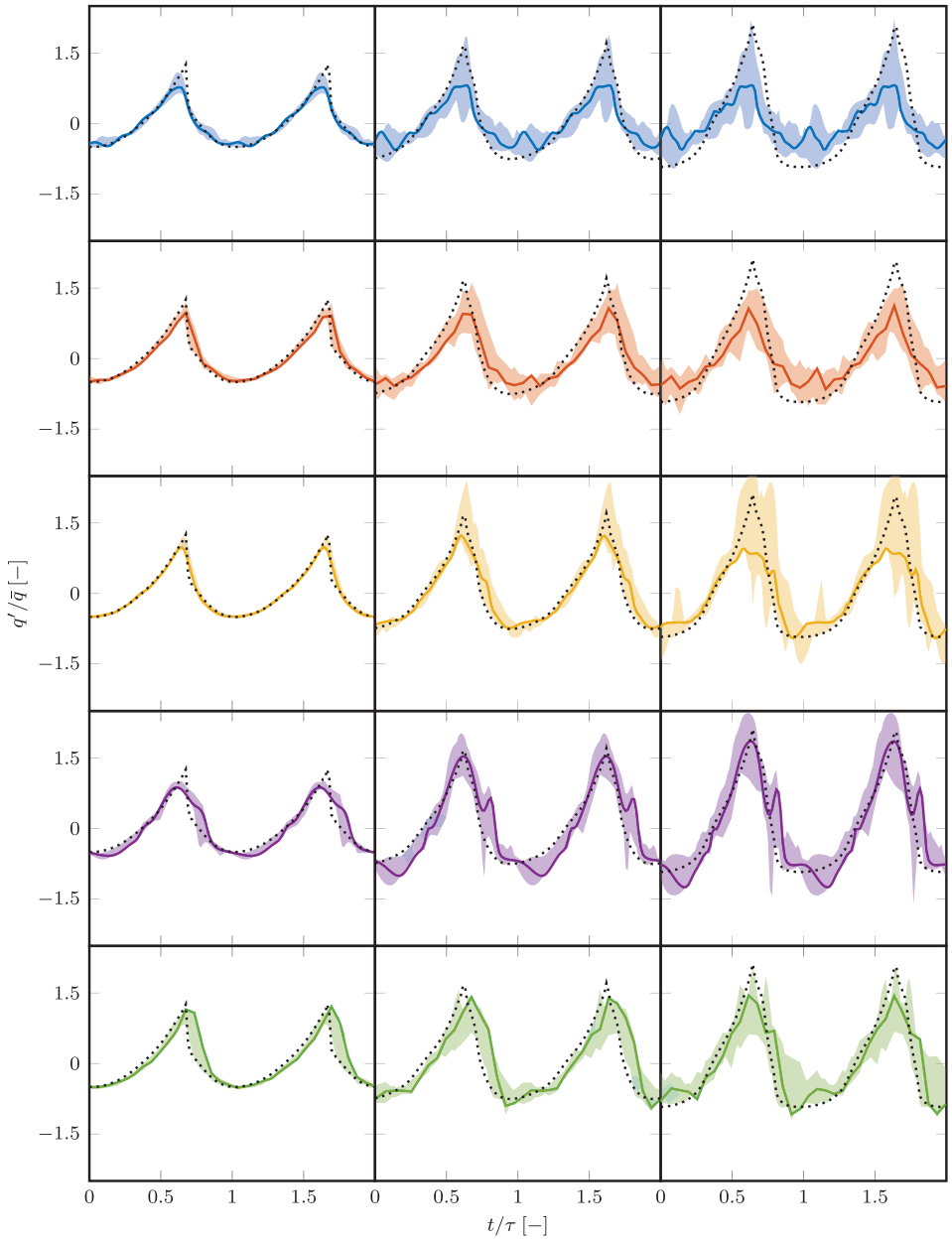

Figure 6. Validation of the response of the 10 optimal ANNs to harmonic forcing in the time domain. Solid line: estimate by the ANN with the highest fit value. Shaded area: bounds of the predictions made by the 10 optimal ANNs. Black dotted line: CFD reference. Forcing frequency: 100 Hz, excitation amplitudes: 50% (left), 100% (middle) and 150% (right), training data sets ordered top to bottom as in Figure 4.

were investigated. The number of unknown parameters of the ANNs varied between 55 and 3801. On each of the five data sets shown in Figure 4, ANNs with the resulting structures were identified. In order to find an optimal ANN for each of the structures, the non-deterministic optimization algorithm was 10 times repeatedly applied. Thereafter, the fit value achieved by each ANN was determined. The 10 ANNs with the highest fit values on each data set were selected. The capability of these optimal ANNs to model the nonlinear flame dynamics is investigated in the next subsections.

4.2. Validation of the forced response

In Figure 5, the FDF deduced from the ANNs is compared against the results obtained from the CFD simulation. An FDF can be deduced from an ANN analogously to the way it is deduced from a CFD simulation or an experiment: at first the ANN is forced with

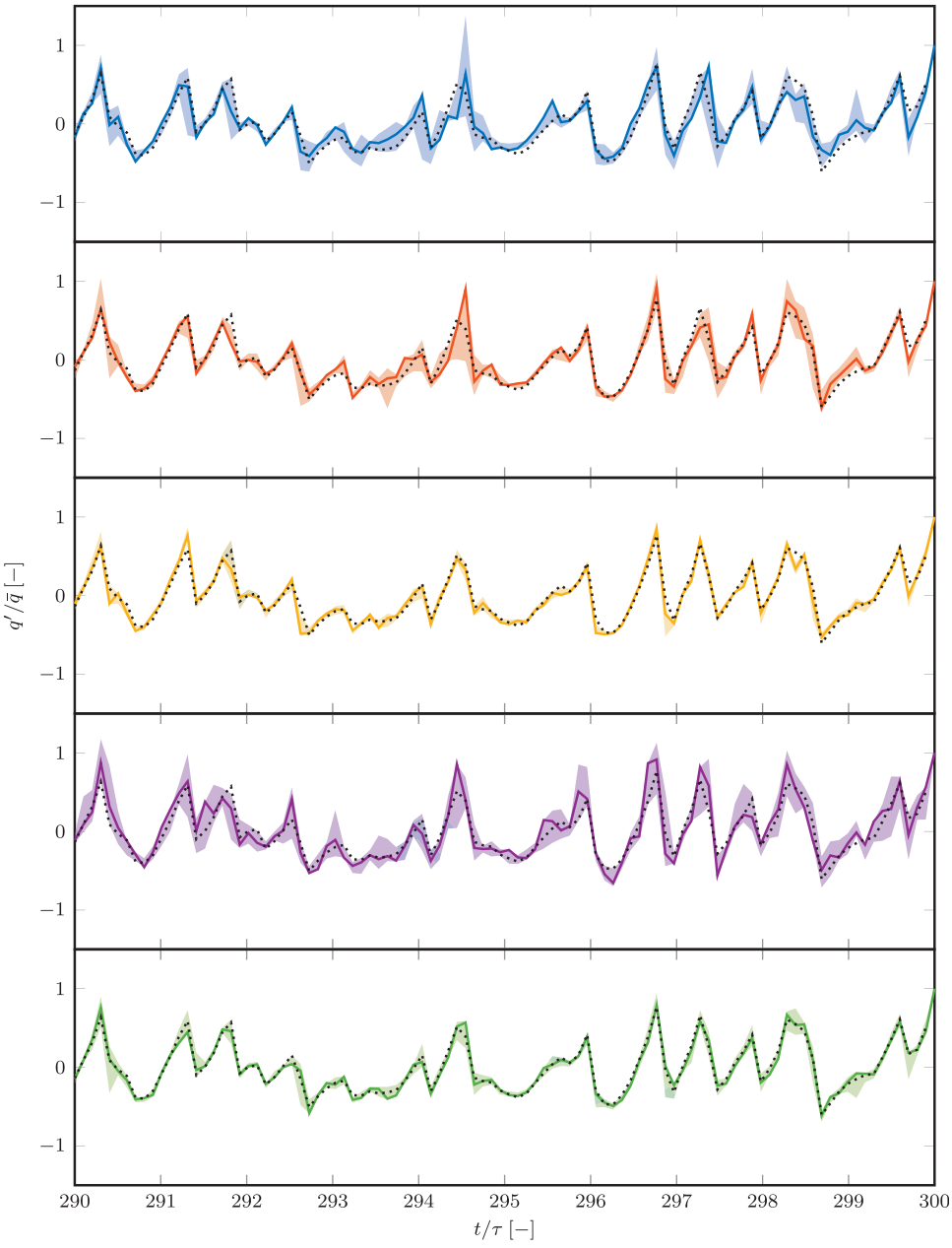

Figure 7. Validation of the forced response of the 10 optimal ANNs against broadband time series. The broadband data are the last 10 t = of data set 5. Solid line: estimate by the ANN with the highest fit value. Shaded area: bounds of the predictions made by the 10 optimal ANNs. Black dotted line: CFD reference. Training data sets ordered top to bottom as in Figure 4.

a harmonic input signal with a specific amplitude and frequency. The output of the ANN is its prediction of the fluctuation of the global heat release rate. The ratio of the Fourier transformed input and output signals at the forcing frequency is the value of the FDF. For frequencies up to 200 Hz, the phases predicted by the ANNS are in excellent agreement with the CFD reference data. Also for higher frequencies, the phase is predicted well. The variance of the results is large only for the highest forcing amplitude considered, i.e. 150% and for the ANNs identified on data set 4. Errors at these high frequencies are expected as the gain of the FDF is very small. The picture is less distinct for the predicted gain. Overall, the low-pass characteristic of the FDF is captured well by the ANNs. The variance of the prediction is quite small for an excitation amplitude of 50% and increases for the higher excitation amplitudes considered. At an excitation amplitude of 50%, a large variance is observed for the ANNs identified on data set 5. This is a problematic observation. It shows that even if very long-time series are available, it cannot be guaranteed that the ANNs identified predict the FDF

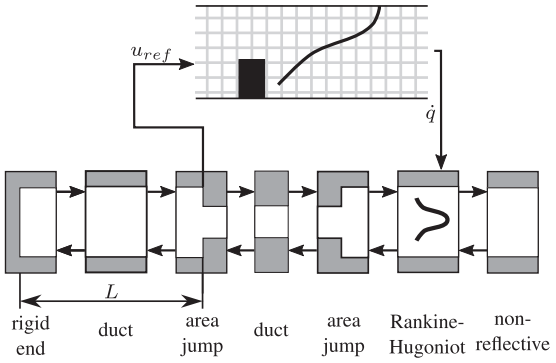

Figure 8. Coupling of the CFD simulation with an acoustic network model to model self-excited thermoacoustic oscillations.

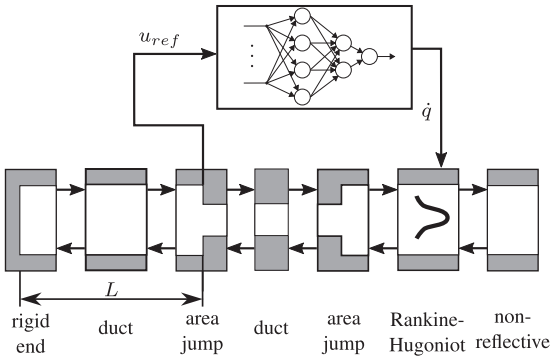

Figure 9. Coupling of an ANN with an acoustic network model to model self-excited thermoacoustic oscillations.

with good accuracy. The results with the ANNs identified on data set 5 improve for higher excitation amplitudes. Here, the prediction is more accurate than the one made by the ANNs identified on the other data sets.

Validating against the FDF allows to compare the results for several different forcing amplitudes and frequencies. However, the analysis is limited to the forcing frequency. This ignores the capability of ANNs to predict also a non-harmonic response of the flame. Therefore, in Figure 6, the response of the optimal ANNs to a harmonic forcing signal is shown in the time domain. The predicted fluctuation of the global heat release rate is validated against the prediction made by the CFD. At an excitation amplitude of 50%, the results are in good agreement with each other and independent from the data set used to identify the ANNs. The variance of the prediction made by the ANNs increases significantly with the excitation amplitude. Up to an amplitude level of 100%, the shape of the response is captured quite well. At 150% amplitude, the peaks of the response are still captured, however, the variance becomes large. The results obtained with data set 4 and data set 5 are slightly more robust. This is expected as these data sets include all excitation amplitudes.

In Figure 7, the ANNS are compared on the last $10t/\tau$ of data set 5. The shape of the response is captured by all sets of ANNs. The ANNs identified on data sets 3 and 5 show the lowest variance. This is because the fit criterion used to select these ANNs contains also the broadband signal shown in Figure 7. The variance of the other sets of optimal neurons is larger. Nevertheless, the main features of the time series are still captured.

4.3. Validation against self-excited oscillations

From the analysis of the forced response, we can conclude that over-fitting was successfully avoided by the procedure applied to obtain the sets of optimal ANNs. However, the analysis depends strongly on the forcing signal used. Therefore, in the present section, the capability of the ANNs identified to predict self-excited thermoacoustic oscillations is investigated.

Both the weakly compressible CFD simulation and the ANNs are models for the flame dynamics of the laminar flame considered. In order to model self-excited thermoacoustic oscillations, they need to be coupled with a model for the acoustics. In Figures 8 and 9, the coupling of the CFD simulation and of an ANN with an acoustic network model is shown, respectively. In Jaensch et al.,[16] the coupling of the CFD and the network model is described in detail. The ANNs are coupled with the acoustic model using Matlab/Simulink.

In Figure 10, the self-excited thermoacoustic oscillations are compared in terms of their RMS values and in terms of the maximal fluctuation of the global heat release rate. The bifurcation parameter is the plenum length, as shown in Figures 1, 8 and 9. At each length investigated, a self-excited oscillation was calculated with all optimal ANNs for $50\,\tau$. As discussed by Jaensch et al.,[16] the thermoacoustic oscillations of the present configurations hardly depend on the initial condition used. In order to minimize the computational effort of the CFD simulation the simulation, was started from a perturbed case. This situation cannot be reproduced with the ANNs. Therefore, we focus the discussion on comparing the fully developed thermoacoustic oscillation. For the results shown in Figure 10, only the last $20\,\tau$ of the $50\,\tau$ time series are used.

At several working points numerical instabilities were observed. One example of such a numerical instability is shown in Figure 11. The oscillation predicted by the ANN develops significantly more slowly than the oscillation predicted by the CFD simulation. This mismatch is due to the different initial conditions used and thus, expected. After about $25\,\tau$, the

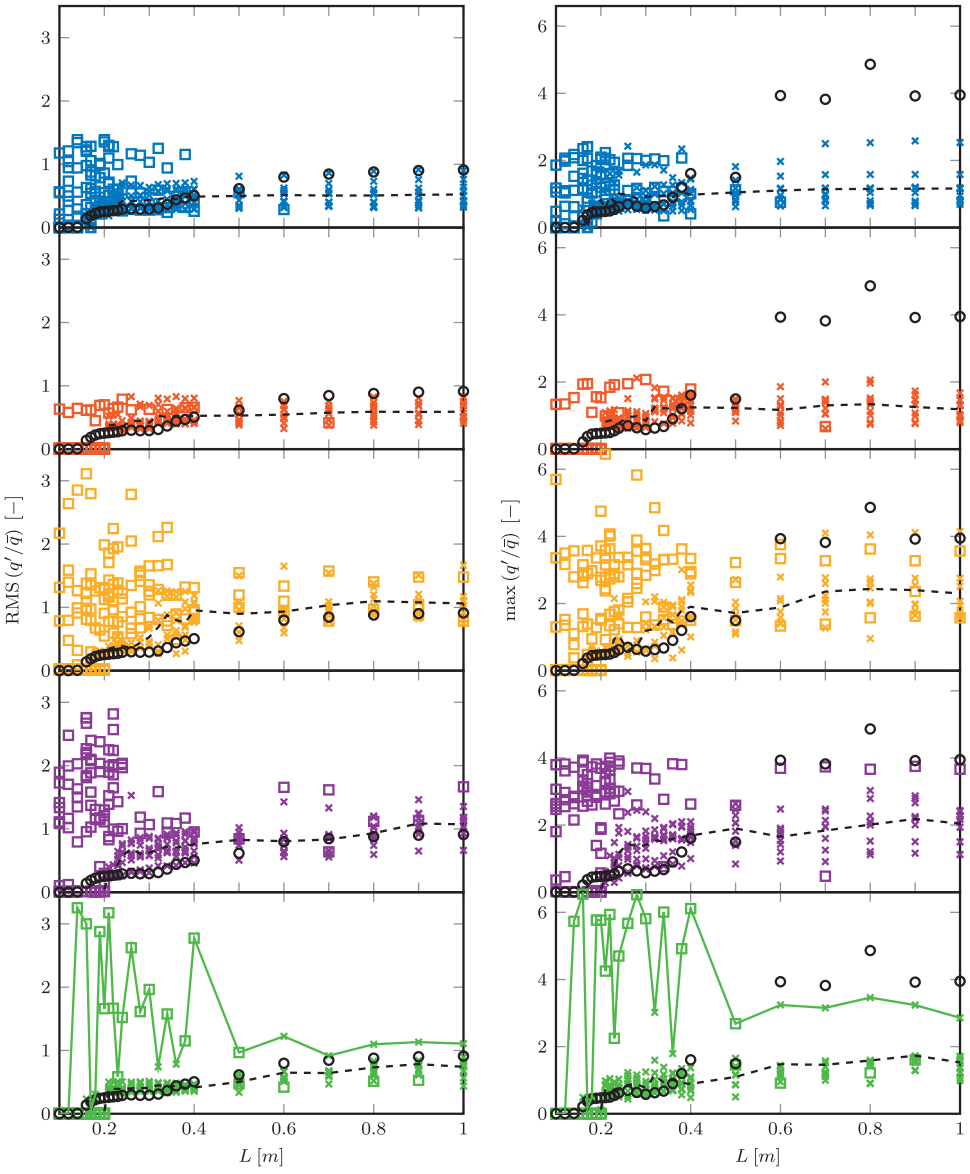

Figure 10. Self-excited thermoacoustic oscillations predicted by the 10 ANNs with the highest fit values on each training set. The training data sets are ordered top to bottom as in Figure 4. Left: comparison in terms of RMS values of the global heat release rate fluctuations; right: comparison in terms of maximum heat release rate fluctuation. Black circles: CFD reference values, colored crosses: solutions oscillating at a dominant frequency f_u in the range of $0\,\text{Hz} < f_u < 800\,\text{Hz}$ predicted by ANNs. These solutions are considered to be physically meaningful. Colored squares: solutions oscillating with a dominant frequency outside of this range. These solutions are considered to be unphysical. Dashed black line: mean value of the physically meaningful solutions predicted by the ANNs. Full green line: connection of the prediction of a selected ANN.

oscillation is in good agreement with the CFD simulation. Unfortunately, numerical errors grow and, after about $35\,\tau$ unphysical oscillations are observed. Such numerical instabilities occur irregularly at different plenum lengths and for different ANNs. These oscillations can be identified as its dominant frequency f_u lies outside the interval $0 < f_u < 800\,\text{Hz}$. In Figure 10, the corresponding data are highlighted with squares.

The variance of the prediction made by the ANNs identified on data set 5 is significantly smaller than the prediction made by the ANNs identified on the other data sets. Only the results of one of these ANNs diverge. This behaviour shows that the prediction of the ANNs improves when longer time series are used to train the ANN. The ANNs identified on data set 5 over-predict the RMS values for short plenum lengths and under-predict the values for long plenum lengths. Nevertheless, the trend of the RMS values is captured. However, the prediction of the maximum heat release fluctuation is poor for long plenum lengths. Only the

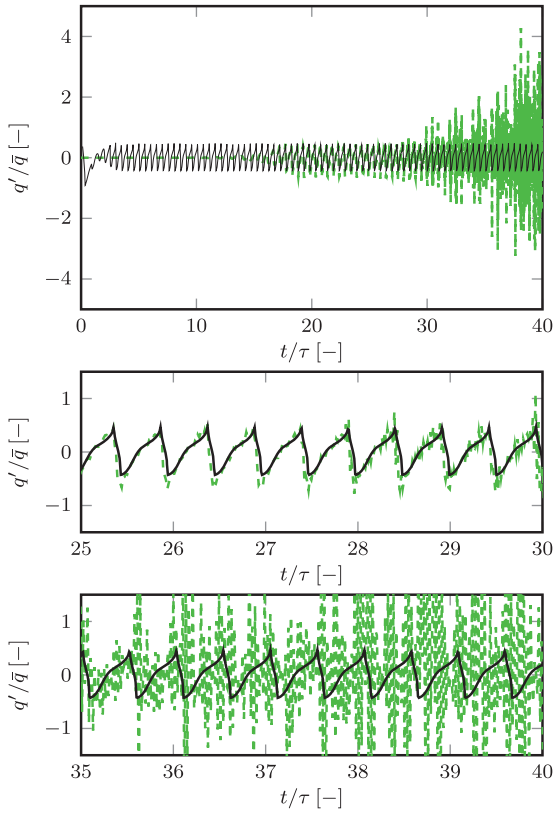

Figure 11. Time series of heat release fluctuation of the self-excited TA oscillations for L = 20 cm. Top: full time series; middle and bottom: zoomed parts of the time series; green-dashed line: prediction of a selected ANN; black line: CFD reference.

prediction of one particular ANN is close to the expected values. In Figure 10, all estimations made by this ANN are connected with a line. This shows that the results of this ANN diverge for short plenum lengths.

5. Conclusion

The capability of ANNs to serve as a model structure in order to deduce nonlinear low-order models of a laminar flame from a CFD simulation was investigated. Via a parameter study a large number of ANNs were identified. A set of 10 optimal ANNs was selected with a fit criterion. The fit criterion only used broadband time series. This allows to evaluate the fit criterion efficiently, since the data used to train the ANNs can be used. Comparing the 10 optimal ANNs allows to estimate the uncertainty of the prediction.

At first the capability of the ANNs to predict the forced response of the flame was analysed. Reasonable agreement was achieved. This shows that over fitting was successfully avoided by the procedure applied to identify and select the optimal ANNs. The validation of the forced response depends strongly on the excitation signal. Therefore, an additional criterion was investigated. The ANNs identified were combined with a thermoacoustic network model in order to model self-excited thermoacoustic oscillations. This comparison is very close to the application. At several working points unphysical numerical instabilities were predicted by the ANNs. It was shown that the variance of the results decreases if very long-time series are used to identify the ANNs. The ANNs identified on the longest of the investigated time series were able to predict the trend of the RMS values. However, the prediction of the maximal fluctuation of the global heat release rate was still poor.

Therefore, we conclude that ANNs, in combination with the identification procedure applied in the present study, do not have the desired properties to deduce nonlinear low-order models from a CFD simulation.

The main problem of the approach is that a good prediction of the forced response does not guarantee a good prediction of self-excited oscillations. This is because the forced response can be analysed for particular excitation signals only. Additionally, in order to obtain an advantage in computational time this signal should be as short as possible. In the present study the longest signal was 30 times longer than a signal needed to determine the FTF. Longer time series would be prohibitively expensive for practical applications.

For the present study the implementation of ANNs provided by Matlab has been used. We consider this implementation as well-established state of the art. The ANN community is rapidly growing and develops a huge number of ANN algorithms, which have their own pros and cons. One of these algorithms may yield better results than the implementation provided by Matlab. This cannot be excluded and is possibly one way to overcome the issues discussed in the present work. Another way to improve the results could be to use different types of excitation signal, e.g. one could use data from simulated self-excited thermoacoustic oscillations. In the author's opinion, however, more sophisticated white- or grey-box models, that account for the physics of the flame dynamics more accurately, are necessary. An additional advantage of grey-box models is that also other information besides the time series of u' and $\dot{q}'$ can be used. For example Jaensch et al.[32] additionally used the acoustic waves emitted by the flame.

Regardless of the way a model was obtained, it should be validated by the systematic procedure proposed in the present study. In particular, the models should be compared in terms of self-excited oscillations.

Acknowledgements

This article has already been published as a non-peer-reviewed publication at the FVV-Frühjahrstagung Turbomaschinen.[35]

Declaration of Conflicting Interests

The author(s) declared no potential conflicts of interest with respect to the research, authorship, and/or publication of this article.

Funding

The author(s) disclosed receipt of the following financial support for the research, authorship, and/or publication of this article: Research Association for Combustion Engines (Forschungsvereinigung Verbrennung e.V – FVV, project number: 6011150). This support is gratefully acknowledged. The authors also gratefully acknowledge the Gauss Centre for Supercomputing e.V. (www.gauss-centre.eu) for funding this project by providing computing time on the GCS Super-computer SuperMUC at Leibniz Supercomputing Centre (LRZ, www.lrz.de).

References

1. Noiray N, Durox D, Schuller T, et al. A unified framework for nonlinear combustion instability analysis based on the flame describing function. *J Fluid Mech* 2008; 615: 139–167.
2. Dowling AP. A kinematic model of a ducted flame. *J Fluid Mech* 1999; 394: 51–72.
3. Cosic B, Moeck J and Paschereit CO. Prediction of pressure amplitudes of self-excited thermoacoustic instabilities for a partially premixed swirl flame. In: *Proceedings of ASME turbo expo* 2013. San Antonio, Texas, USA: The American Society of Mechanical Engineers GT2013-94160, 2013.
4. Krediet HJ, Beck CH, Krebs W, et al. Saturation mechanism of the heat release response of a premixed swirl flame using LES. *Proc Combust Inst* 2013; 34: 1223–1230.
5. Han X and Morgans AS. Simulation of the flame describing function of a turbulent premixed flame using an open-source LES solver. *Combust Flame* 2015; 162: 1778–1792.
6. Han X, Li J and Morgans AS. Prediction of combustion instability limit cycle oscillations by combining flame describing function simulations with a thermoacoustic network model. *Combust Flame* 2015; 162: 1778–1792.
7. Moeck J and Paschereit C. Nonlinear interactions of multiple linearly unstable thermoacoustic modes. *Int J Spray Combust Dyn* 2012; 4: 1–28.
8. Orchini A, Illingworth S and Juniper M. Frequency domain and time domain analysis of thermoacoustic oscillations with wave-based acoustics. *J Fluid Mech* 2015; 775: 387–414.
9. Kashinath K, Hemchandra S and Juniper MP. Nonlinear phenomena in thermoacoustic systems with premixed flames. *J Eng Gas Turb Power* 2013; 135: 061502.
10. Kashinath K, Waugh IC and Juniper MP. Nonlinear self-excited thermoacoustic oscillations of a ducted premixed flame: bifurcations and routes to chaos. *J Fluid Mech* 2014; 761: 399–430.
11. Kashinath K, Hemchandra S and Juniper MP. Nonlinear thermoacoustics of ducted premixed flames: The influence of perturbation convection speed. *Combust Flame* 2013; 160: 2856–2865.
12. Chakravarthy SR, Balaji C, Katreddy RKR, et al. A framework for numerical simulation of turbulent incompressible unsteady flame dynamics coupled with acoustic calculations in time and frequency domains. In: *n3l – International summer school and workshop on non-normal and nonlinear effects in aero- and thermoacoustics*. Munich, Germany: Technische Universität München, 2013, p.12.
13. Moeck J, Scharfenberg C, Paschereit O, et al. A zero-Mach solver and reduced order acoustic representations for modeling and control of combustion instabilities. In: *Active flow control II, notes on numerical fluid mechanics and multidisciplinary design*, Springer-Verlag Berlin Heidelberg, Germany, Vol. 108, 2010, pp.291–306.
14. Schuermans B, Luebcke H, Bajusz D, et al. Thermoacoustic analysis of gas turbine combustion systems using unsteady CFD. In: *Proceedings of ASME turbo expo 2005*. GT2005-68393. Reno, Nevada: ASME, p.2005.
15. Wall CT. *Numerical methods for large Eddy simulation of acoustic combustion instabilities*. PhD Thesis, Stanford University, 2005.
16. Jaensch S, Merk M, Gopalakrishnan E, et al. Hybrid CFD/ low-order modeling of nonlinear thermoacoustic oscillations. In: *Proceedings of the Combustion Institute*, Vol. 36, 2017, pp. 3827–3834.
17. Polifke W. Black-box system identification for reduced order model construction. *Ann Nucl Energy* 2014; 67C: 109–128.
18. Isermann R and Münchhof M. *Identification of dynamical systems: An introduction with applications*. Advanced textbooks in control and signal processing. Berlin and Heidelberg: Springer-Verlag, 2010.
19. Tangirala AK. *Principles of system identification: Theory and practice*. Boca Raton, Florida, USA: CRC Press, 2014.
20. Nelles O. *Nonlinear system identification: From classical approaches to neural networks and fuzzy models*. Springer-Verlag Berlin Heidelberg, Germany, 2001.
21. Selimefendigil F, Föller S and Polifke W. Nonlinear identification of the unsteady heat transfer of a cylinder in pulsating crossflow. *Comput Fluids* 2012; 53: 1–14.
22. Selimefendigil F and Polifke W. A nonlinear frequency domain system model with coupled modes for limit cycle prediction of thermoacoustic systems. *Int J Spray Comb Dyn* 2011; 3: 303–330.
23. Selimefendigil F. *Identification and analysis of nonlinear heat sources in thermo-acoustic systems*. PhD Thesis, TU München, 2010.
24. Zhang Z, Guan D, Zheng Y, et al. Characterizing premixed laminar flame–acoustics nonlinear interaction. *Energy Convers Manage* 2015; 98: 331–339.
25. Blonbou R, Laverdant A, Zaleski S, et al. Active adaptive combustion control using neural networks. *Combust Sci Technol* 2000; 156: 25–47.
26. Blonbou R, Laverdant A, Zaleski S, et al. Active control of combustion instabilities on a rijke tube using neural networks. *Proc Combust Inst* 2000; 28: 747–755.
27. Vaudrey MA and Saunders WR. Control of combustor instabilities using an artificial neural network. In:

Proceedings of ASME TURBO EXPO, Munich, Germany, 2000-GT-0529, 2000.
28. Kornilov VN, Rook R, ten Thije Boonkkamp JHM, et al. Experimental and numerical investigation of the acoustic response of multi-slit Bunsen burners. *Combust Flame* 2009; 156: 1957–1970.
29. Duchaine F, Boudy F, Durox D, et al. Sensitivity analysis of transfer functions of laminar flames. *Combust Flame* 2011; 158: 2384–2394.
30. Bomberg S, Emmert T and Polifke W. Thermal versus acoustic response of velocity sensitive premixed flames. In: *35th symposium on combustion*. Vol. 35, San Francisco, CA: The Combustion Institute, 2014.
31. Blumenthal RS, Subramanian P, Sujith R, et al. Novel perspectives on the dynamics of premixed flames. *Combust Flame* 2013; 160: 1215–1224.
32. Jaensch S, Emmert T, Silva CF, et al. A grey-box identification approach for thermoacoustic network models. In: *Proceedings of ASME turbo expo*. Düsseldorf, Germany: The American Society of Mechanical Engineers, GT2014-27034, 2014.
33. Silva CF, Jaensch S, Emmert T, et al. On the autoregressive behavior of the intrinsic thermoacoustic feedback loop observed in premixed flames. In: *22nd International congress on sound and vibration (ICSV22)*. Florence, Italy: The International Institute of Acoustics and Vibration (IIAV), 2015.
34. Föller S and Polifke W. Advances in identification techniques for aero-acoustic scattering coefficients from large Eddy simulation. In: *18th International congress on sound and vibration (ICSV18)*. Rio de Janeiro, Brazil: The International Institute of Acoustics and Vibration (IIAV), 2011.
35. Jaensch S and Polifke W. On the uncertainty encountered when modeling self-excited thermoacoustic oscillations with artificial neural networks. In: *International symposium on thermoacoustic instabilities in gas turbines and rocket engines*. Garching, Germany: Technische Universität München (TUM), 2016.